Discover Geoscience

RESEARCH Open Access

Characterization of groundwater flow in the cuesta reverse from structural analysis and electrical resistivity tomography

César Augusto Moreira[1], Leonides Guireli Netto[2*], Stephanie de Freitas Schorcht[3], Iata Anderson de Souza[1], Henri Masquelin[4], Marco Antonio Fontoura Hansen[5] and José Pedro Rebés Lima[5]

*Correspondence:
Leonides Guireli Netto
leonidesnetto@ipt.br
[1]Department of Geology, Geosciences and Exact Sciences Institute, São Paulo State University, Rio Claro, São Paulo State, Brazil
[2]Cities, Infrastructure and Environment Department, Institute for Technological Research, São Paulo, Brazil
[3]Graduation program in Geosciences and Environmental Science, Geosciences and Exact Sciences Institute, São Paulo State University, Rio Claro, São Paulo State, Brazil
[4]Instituto de Ciencias Geológicas, Universidad de la Republica, Montevideo, Uruguay
[5]Pampa Federal University, Caçapava do Sul, Rio Grande do Sul State, Brazil

Abstract
Water availability and quality have been identified as essential for human development, encompassing sectors such as agriculture, industry, and public supply. This study adopted a multidisciplinary approach, integrating geophysical methods, focusing on electrical resistivity tomography, and structural surveys to investigate a confined fractured aquifer in the Serra do Itaqueri region, known for its complex and diverse geology. Located on the eastern edge of the Paraná Basin, this region exhibited rugged terrain predominantly composed of sandstones from the Botucatu Formation and basalts from the Serra Geral Formation, in addition to fracture and fault systems controlling subsurface flow. The results indicated recharge and discharge zones associated with tectonic structures, such as a NE-SW-oriented reverse fault that acted as a hydraulic barrier in certain sections. 2D and 3D electrical resistivity models revealed significant contrasts between saturated and unsaturated zones, emphasizing the recharge zone's vulnerability to human activities. The results underscored the importance of electrical tomography as a tool for aquifer characterization and the need for conservation strategies to preserve water resources in environmentally fragile areas.

Keywords Groundwater flow dynamics, Hydrogeophysics, Structural geology, Fractured aquifer, Water resource management

1 Introduction

The availability and quality of water are fundamental to human development, covering sectors such as agriculture, industry, energy generation and public supply. The intensification of these activities, driven by population expansion, has significantly increased the demand for water, highlighting the need to explore alternative sources and protect existing resources. Although surface resources are widely used, their greater vulnerability to contamination compared to groundwater often requires more complex and costly treatments [1]. Worldwide, around 2.5 billion people depend on aquifers as their primary source of drinking water, and the demand for these resources continues to grow due to

the intensification of agriculture, industry and domestic use [2, 3]. In Brazil, groundwater has a strategic role to fulfill in terms of water supply, since 40% of municipalities depend exclusively on these resources. However, activities such as intensive agriculture have threatened the quality of these reserves due to the indiscriminate use of agrochemicals and the over-exploitation of aquifers [4], which compromises recharge and reduces discharge into associated rivers [5, 6]. Although aquifers are less susceptible to contamination, once polluted, their treatment is more costly and complex than that of surface resources [7, 8].

Considering its importance, understanding the processes that regulate the occurrence and dynamics of groundwater is essential, especially in the context of recharge and discharge zones [9, 10]. The recharge zone is the area where surface water infiltrates, reaching the saturated zone, while the discharge zone is where groundwater returns to the surface, often in lower altitude regions, such as springs [11, 12]. In rocky settings, groundwater can be confined in porous aquifers, which are common in sedimentary rocks, or in fractured aquifers, which depend on the presence of fractures to form porous and permeable spaces in crystalline rocks, such as igneous and metamorphic rocks [13, 14]. The identification and characterization of these aquifers, especially the fractured ones, require multidisciplinary approaches that integrate structural field surveys and geophysical methods. In this context, electrical tomography can be an interesting tool in the investigation of fractured aquifers, due to its ability to provide variations in the electrical resistivity of the subsoil [15]. These variations can be associated with different hydrogeological conditions, such as the presence of water in fractures or more resistive zones, which indicate more compact materials or lower saturation. In general, more saturated environments, such as water-filled fractures, tend to have low electrical resistivity, while drier or less permeable zones are characterized by higher electrical resistivity [16].

Recent studies reinforce the effectiveness of the hydrogeophysical approach in complex environments [17–19]. This type of environment is challenging due to the heterogeneity of geological and hydrogeological conditions [5, 19]. In Brazil, the application of hydrogeophysics to study fractured aquifers has become more prominent in the context of crystalline rocks in the Northeast and Southeast, regions where dependence on groundwater is significant [20]. Studies such as [21, 22] have used electrical resistivity tomography to identify fracturing zones in granites and gneisses, highlighting the importance of these structures for the formation of productive aquifers in semi-arid and mountainous regions [23, 24]. Internationally, the technique has also been widely applied in areas with similar geological characteristics, such as sub-Saharan Africa and India, where fractured aquifers are vital for water supply, but often lack detailed characterization due to the complexity of the rock formations [25–31]. Studies in areas such as the Rift Valley in Kenya and the semi-arid regions of India have shown how hydrogeophysics, especially electrical tomography, can help map fractures and identify recharge and discharge zones for these aquifers in challenging environments [32–35]. demonstrated that the integration of electrical tomography with structural surveys can delimit fracturing zones in metamorphic rocks, making it possible to infer the hydraulic connectivity of aquifers. Similarly, work such as that by [36] applied electrical tomography to map aquifers in fault zones, revealing the influence of tectonic structures on groundwater recharge and storage. In tropical regions, as demonstrated by [37], the combination

of geophysical methods, including electrical tomography, revealed saturation patterns related to seasonal variations in precipitation and land use. These results highlight the potential of the approach to identify promising sites for well drilling and groundwater resource management.

In this study, compass measurements were taken of the orientation of the rock fractures, along with geophysical investigations using electrical resistivity tomography. The work was carried out during the dry season, with the aim of understanding the interactions between groundwater and surface water and assessing the viability of the fractured aquifer as a strategic water source for the region. The main objective of this research is to characterize the groundwater flow dynamics in the fractured aquifer by integrating structural geology and hydrogeophysical methods. Specifically, the study aims to identify the influence of tectonic structures on groundwater movement, delineate recharge and discharge zones, and evaluate the hydrogeological potential of the investigated aquifer. The structural survey was carried out in an outcrop located in the Serra Geral Formation, in the northern part of the basin, where volcanic rocks associated with fissural magmatism can be seen. The structural data collected in the field was processed, generating pole diagrams and stereograms illustrating the directions of the fractures and their respective dip angles. This structural information was integrated with the results of the geophysical investigations, allowing for the interpretation of the sections and the construction of three-dimensional electrical resistivity models obtained using the electrical resistivity tomography technique. The combination of these approaches made it possible to identify zones with greater permeability associated with the fractures, as well as providing a more detailed overview of the spatial distribution of hydrogeological characteristics, which are essential for understanding the dynamics of the fractured aquifer in the study area.

2 Study area

The study area is located on the edge of the Serra de Itaqueri, a regional geological formation on the edge of the Paraná Basin, situated approximately 200 km northwest of the city of São Paulo, the state capital (Fig. 1). This area has intense agricultural activity, especially sugar cane production, whose water demand is high both for irrigation and industrial processing [38]. This significant dependence on water resources makes hydrogeological studies essential to ensure the sustainability of groundwater use, especially in fractured aquifers, where water availability is directly related to the distribution and connectivity of fractures. Furthermore, understanding the recharge and discharge dynamics of aquifers in the region is important not only to meet the demands of the agricultural sector, but also to ensure the quality and quantity of water available for human and industrial consumption, mitigating environmental and social impacts in the long term [39, 40].

The geological context of the edge of the Serra de Itaqueri is marked by the interaction between the sedimentary rocks of the Paraná Basin and the crystalline rocks of the Precambrian basement, a configuration that favors the formation of fractured aquifers. The hydrogeological conditions of the study area are strongly influenced by its geological setting. The fractured basalt of the Serra Geral Formation, in particular, plays an important role in the storage and flow of groundwater. Fractures in the basalt provide pathways for the movement of groundwater, which is crucial for the sustainability of the region's water

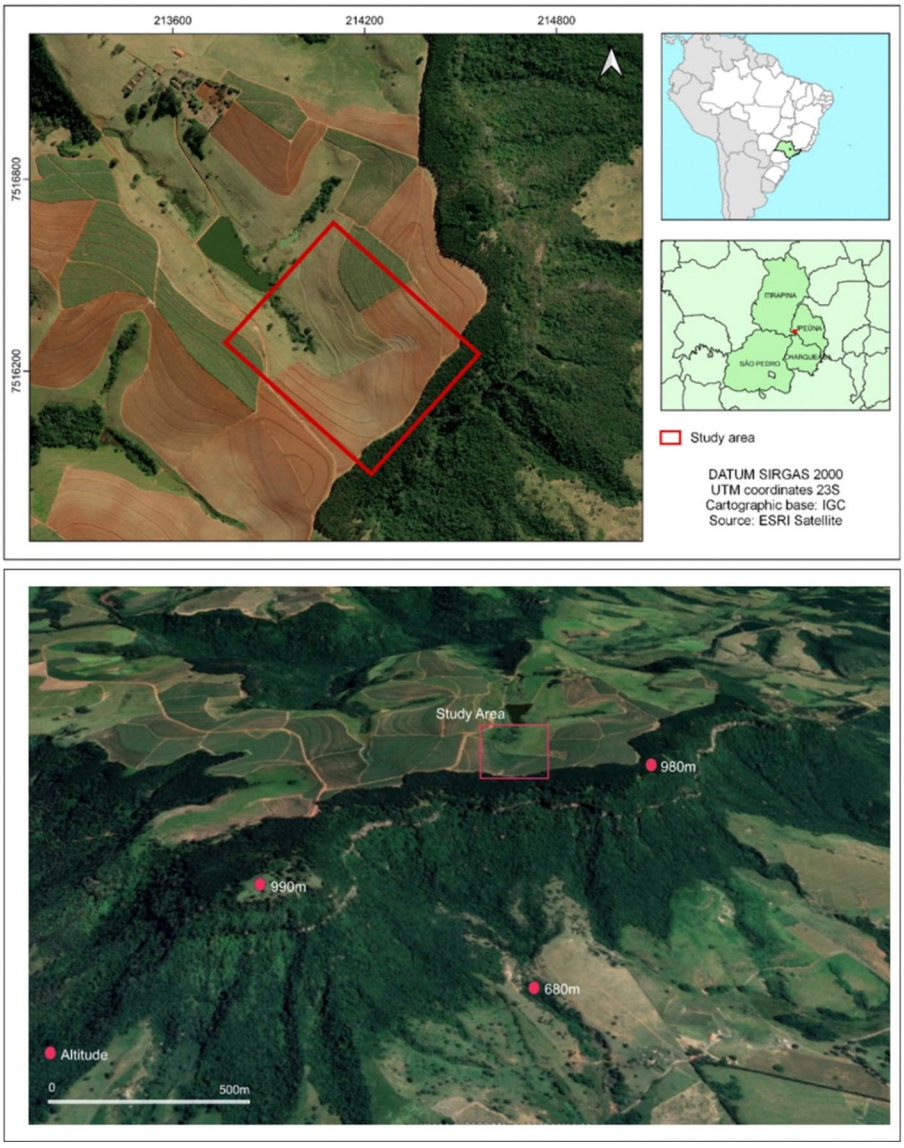

Fig. 1 Location map of the study area in the Serra de Itaqueri, combined with a three-dimensional image of the cuesta front in the same region. The visualization was generated from Google Earth data

resources, especially during periods of high demand, such as the dry season. In addition, the sandstones of the São Bento Group, especially the Botucatu Formation, are known to have moderate to high permeability, facilitating groundwater flow in areas where they are not deeply weathered or fractured. The interactions between these geological units, especially where the basaltic and sandstone layers are in contact, create zones of high permeability that are essential for groundwater recharge and discharge. In addition, tectonic activity in the region, in particular faults and fractures, contributes to the creation of preferential flow paths and affects the spatial distribution of aquifers. Understanding these hydrogeological characteristics is fundamental to assessing the potential for extraction and sustainable management of groundwater in the region. The Paraná Basin, with an area of approximately 1.5 million square kilometers, covers large areas of Brazil and neighboring countries such as Paraguay, Argentina and Uruguay [41]. This sedimentary basin records geological events from the Paleozoic to the Cenozoic and includes

units with high hydrogeological importance, such as the sandstones of the São Bento Group and the basaltic flows of the Serra Geral Formation. This diverse hydrogeological scenario makes the Serra de Itaqueri region an important object of study, both for its water potential and for the challenges related to the sustainable management of underground resources in an area of increasing anthropogenic pressure (Fig. 2).

The São Bento Group, made up of the Pirambóia and Botucatu Formations, is characterized by eolian sediments that reflect different paleoenvironmental conditions. The Pirambóia Formation has sandstones of varying color, fine to medium grain size and clay intercalations, associated with humid eolian systems with the presence of humid interdunes at the base, transitioning to a drier environment at the top [43]. In turn, the Botucatu Formation is made up of medium to fine sandstones, well-selected and highly mature, which demonstrate the deposition of a dry desert environment in extensive dune fields. The discordant contact between these formations reflects tectonic and climatic changes during the Mesozoic [44].

The Serra Geral Formation, located at the top of the São Bento Group sedimentary sequence, is made up of basaltic flows generated by fissural magmatism related to the separation of Gondwana. Dating back between 133 and 132 million years [45], these basaltic rocks are recognized for their hydrogeological properties, such as the formation of fractured aquifers, often intercalated with sandstones of the Botucatu Formation. In addition, the Serra Geral Formation represents one of the largest magmatic provinces on the planet, standing out for its regional impact on hydrogeological behavior [46]. In the Cenozoic, deposits of the Bauru Group and undifferentiated surface cover the older formations, marking a phase of sedimentation in predominantly fluvial and aeolian environments. These more recent deposits play a fundamental role in recharging and storing groundwater.

Locally, the geology of the Serra de Itaqueri shows clear evidence of the interactions between the structural and lithological processes that have shaped the region. One example is the basalt outcrop of the Serra Geral Formation, located on a road on the southwestern flank of the valley (Fig. 2). This outcrop shows different degrees of weathering in the basalt, which reflects the combined influence of climatic, structural and lithological factors in the evolution of the terrain. At the base, the basalt is little modified, with well-preserved columnar disjunctions (Fig. 2a), typical of the Serra Geral

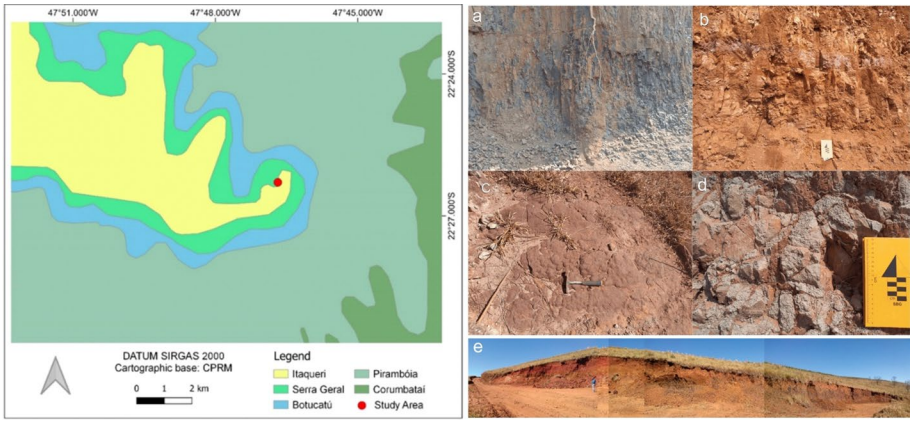

Fig. 2 Regional geological map. (Source: [42] and outcrop near the geophysical lines, with the separation of the layers: **a** columnar disjunction, **b** altered basalt, **c** laterite and **d** weathering profile

Formation. As the topography progresses, there is an increase in the alteration of the basalt, culminating in a completely changed state, where the disjunctions are no longer visible (Fig. 2b). On top of this layer is a laterite (Fig. 2c), which reflects intense weathering processes, and, at the top, a more advanced alteration profile (Fig. 2d).

These local characteristics are directly related to the hydrogeological and structural context of the region. Tectonic structures, such as the faults and lineaments mentioned above, not only control the relief and drainage pattern, but also influence the exposure and degree of weathering of the rocks. Basalt that is little modified at the base, with preserved disjunctions, can act as a potential reservoir in fractured aquifers, allowing for the storage and flow of groundwater. The upper, more weathered layers, on the other hand, may be less permeable, acting as barriers or water retention zones. In addition, the presence of laterite and the alteration profile at the top shows the influence of climatic processes on soil development, which directly affects water recharge.

3 Methods

3.1 Structural characterization: regional and local analysis of lineaments and fractures

Regional structural data was acquired using Shuttle Radar Topography Mission (SRTM) images, at a resolution of 1 arc-second (30 m), obtained from the US Geological Survey (USGS) open data library. The methodology used followed the principles described by [47], who proposed the extraction of lineaments from aerial images. In this study, lineaments were extracted directly from SRTM images based on geomorphological features that reflect structural characteristics, such as textural differences, ridge and valley alignments, elongated coastlines, escarpment segments and linear depressions. For the analysis, a Digital Elevation Model (DEM) was generated in Global Mapper 12.0 software, with the application of color palettes to facilitate the identification of relief. The DEM was exported as a raster image and processed in QGIS 3.14, where the lineaments were digitized manually, creating a vector layer. This layer was transferred to AutoCAD 2018 software, where rosette diagrams of cumulative length and cumulative frequency were generated. The final map was edited and produced in QGIS 3.14, integrating the results into the regional geomorphological context. In the field activity, fracture and bedding measurements were collected in an outcrop located near the geophysical prospecting area, as well as in two caves in the region. These measurements were taken using a Clar-type geological compass, which allows the orientation and inclination of structures to be recorded. The aim was to understand the behavior of the fractures in the fractured aquifer, which is fundamental for evaluating the preferential underground flow paths and the mechanisms of water recharge and discharge. The data collected in the field was processed using Stereonet 10.2.9 software to generate stereograms and pole contour diagrams. This analysis made it possible to identify local structural patterns and their relationship with previously mapped regional lineaments.

3.2 Electrical resistivity tomography (ERT)

Electrical resistivity tomography is a geophysical technique that allows the generation of two-dimensional (2D) or three-dimensional (3D) models of the subsoil, based on electrical resistivity measurements. It uses electrodes to inject electric current into the ground (current electrodes) and measure the potential difference (potential electrodes). These electrodes are arranged along a profile and moved laterally, allowing data to be

collected at different depths and areas. By adjusting the spacing between the electrodes, it becomes possible to correlate depth and lateral extent, offering a detailed view of the heterogeneities in the geological environment from the interpretation of variations in electrical resistivity [48, 49]. This technique stands out for its versatility and is widely used in hydrogeological, environmental and geotechnical research [50, 51]. In aquifers, for example, it is possible to identify saturated or unsaturated zones, as well as contrast bodies of groundwater with underlying rocks, due to their higher electrical conductivity [20, 52, 53]. In crystalline rock terrain, the technique is especially useful for detecting fluid-filled fractures, where the resistivity contrast is directly related to the nature and amount of fluid present [12, 16, 54].

In this study, 8 lines of electrical resistivity tomography were carried out using the Schlumberger array, due to its high sensitivity to vertical variations in resistivity [55]. This array is characterized by the use of two current electrodes (A and B) and two potential electrodes (M and N) positioned symmetrically in relation to the center of the profile. The main advantage of this arrangement lies in the ability to obtain depth readings with good vertical resolution, even in terrain with complex electrical variability [56]. The lines set up in the study comprised 7 profiles perpendicular to the drainage, 400 m long and spaced 50 m apart, as well as a 330-meter longitudinal line (Fig. 3). With a spacing of 10 m between electrodes, it was possible to reach depths of up to 100 m in the central region of the lines. This configuration made it possible to capture data with excellent resolution for analyzing the saturated and unsaturated zones, which is essential for understanding local hydrogeology [15]. The Terrameter LS resistivity meter, produced by ABEM Instrument, was used to acquire resistivity measurements. This equipment has

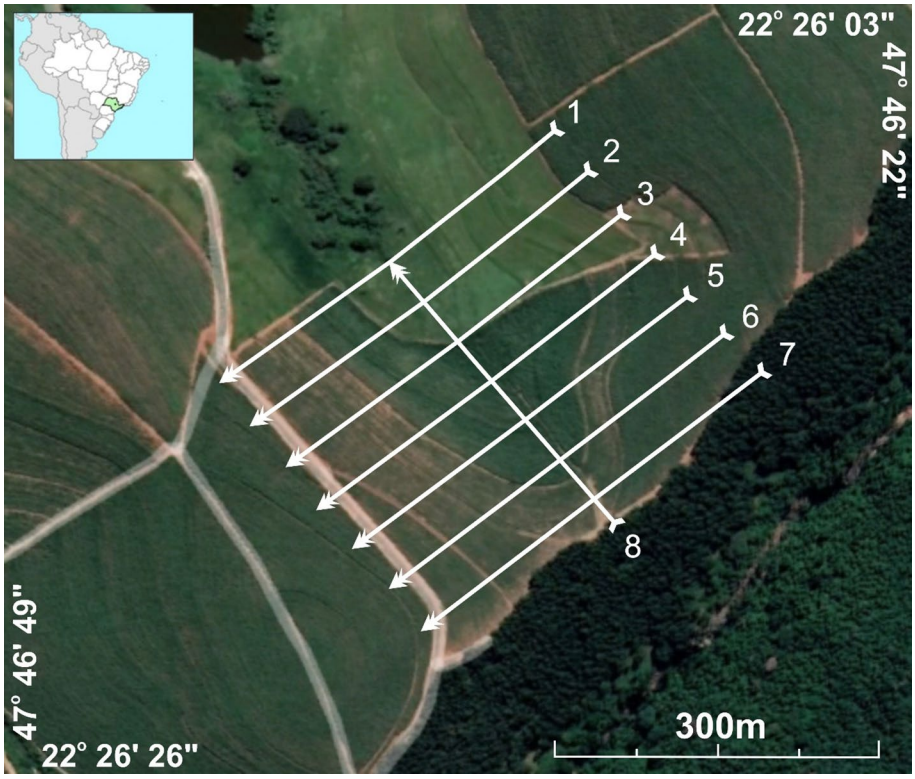

Fig. 3 Distribution of the electrical resistivity tomography lines, indicating the direction in which the data was obtained, from NE to SW and, in the case of the T line, from NW to SE

250 W of power, configuration for up to 12 reading channels, current of up to 2500 mA and resolution of 1 μV [57].

Processing the data collected involved several stages to ensure the accuracy of the models generated. Initially, the data was organized and checked to identify and correct possible collection errors [58]. During this stage, spurious data that could introduce distortions in the results was removed. In addition, the topographic data for each line was integrated to improve the accuracy of the sections generated [59, 60]. Data inversion was carried out using the RES2DINV software (version 3.53), which employs the smoothness-constrained least squares method. This algorithm makes it possible to calculate adjusted two-dimensional models, reducing discrepancies between the observed and calculated data, while smoothing out abrupt variations that do not represent the real characteristics of the environment under investigation [48]. In this study, a total of 10 iterations were performed during the inversion process. The Root Mean Square (RMS) error, which quantifies the difference between the observed and calculated apparent resistivities, was used to evaluate the quality of the inversion [49]. All obtained RMS values were below 4, indicating a good fit between the model and the field data. This low RMS error suggests that the collected data was of high quality and that the processing steps effectively minimized inconsistencies, leading to reliable resistivity models. For three-dimensional (3D) visualizations, the 2D sections obtained were integrated and interpolated in the Oasis Montaj software (Geosoft). The interpolation was carried out using the kriging method, ensuring smoothing of the values and accurate representation of the resistivity variations throughout the investigated space [61]. This procedure resulted in 3D models that were fundamental for interpreting the distribution of hydrogeological properties and the resistivity contrasts associated with the different layers of the subsoil.

4 Results

4.1 Structural characterization: regional and local analysis of lineaments and fractures

Regional structural lineaments represent rectilinear expressions of geological structures that affect the surface of the terrain, and are identified in aerial and satellite images. In order to understand the structural pattern of the Serra de Itaqueri region and correlate it with field structural data and geophysical lines, a lineament map was drawn up based on SRTM data. Analysis of these lineaments enabled the generation of rosette diagrams for cumulative length and cumulative frequency (Fig. 4), which helped interpret the structural pattern influencing the local relief and drainage. The results show that the NW lineaments, especially N60-70 W, are more significant in terms of both length and frequency. NS directions are also relevant, especially in absolute frequency, which is in line with the literature, which associates these features with rupile structures reactivated in recent geological times, with a significant influence on the compartmentalization of the relief and river systems [62, 63]. NE lineaments, such as N40-50E and N60-70E, are shorter in length but high in frequency and correlate with phases of Cenozoic sedimentation. On the other hand, E-W lineaments, although short and less frequent, play an important role in the dissection of the relief.

In the local structural geological context, structural data was collected in an area close to the electrical resistivity tomography lines to complement the study and assess the influence of the structural context on underground flow. The main outcrop analyzed is

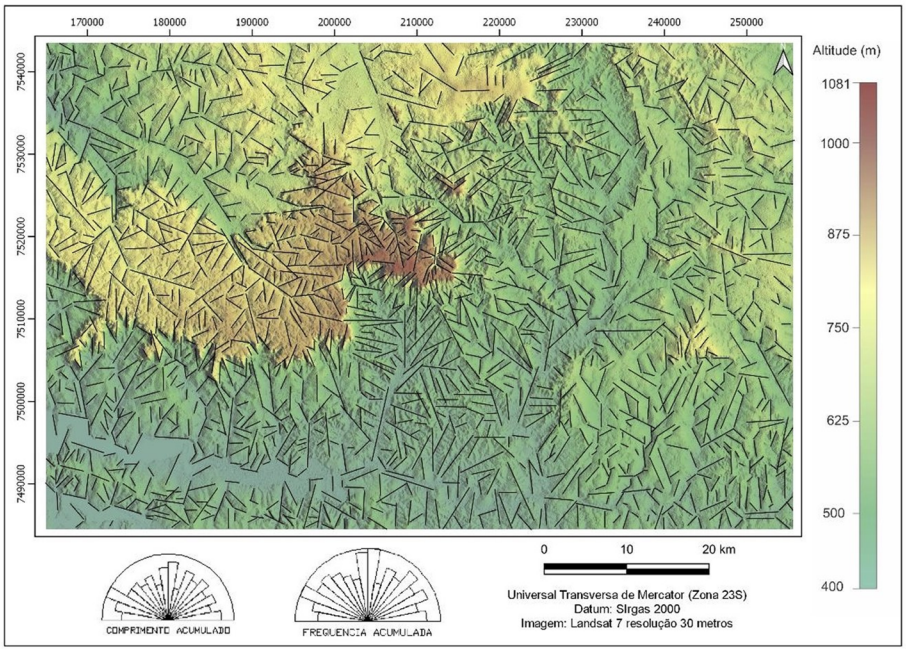

Fig. 4 SRTM digital elevation model with tectonic lineaments of the study area and rosette diagrams of accumulated frequency and length

located on the southwest flank of the valley and presents a lithological sequence with different degrees of weathering: slightly altered basalt with columnar disjunctions, highly weathered basalt, laterite and sandy material. In the slightly weathered basalt, the columnar disjunctions show high-angle fractures, with no obvious preferential direction. The stereograms show various directions, such as NNW-SSE, NE-SW, NW-SE, WNW-ESE and E-W (Fig. 5a). In the well-altered basalt, the disjunct structures are less visible, but the NE-SW and NW-SE directions remain prominent (Fig. 5b). This pattern suggests that the regional structural influence persists even with weathering. At the top of the alteration profile, fractures observed in the laterite show similar directions (NW-SE and NNE-SSW), with a high dip angle (Fig. 5c). This indicates that these structures may be the result of tectonic stresses subsequent to the formation and weathering of the rock. Analyses in two caves in the region, including the largest mapped cave, revealed fracture patterns in sandstone, with planes in multiple directions and medium to high angle dips. Highlighted beams include NE-SW and NW-SE directions (Fig. 5d). These patterns are consistent with regional lineaments and reinforce the role of structural control in drainage, relief and weathering and erosion processes.

4.2 Electrical resistivity tomography (ERT)

The geophysical data obtained from the electrical resistivity tomography (ERT) showed good quality, with a low percentage of error, as evidenced by the low value of the Root Mean Square Error (RMS) in all the lines processed. The RMS is a measure that quantifies the difference between the observed data and the modeled results, and is used to assess the accuracy of the model's fit to the real data. The 2D inversion models were generated from electro-resistivity lines with a NE-SW orientation, perpendicular to the surface drainage line. In addition, an additional line (T-Line), oriented in a NW-SE direction, was used to complement the data, providing a more detailed view of the study

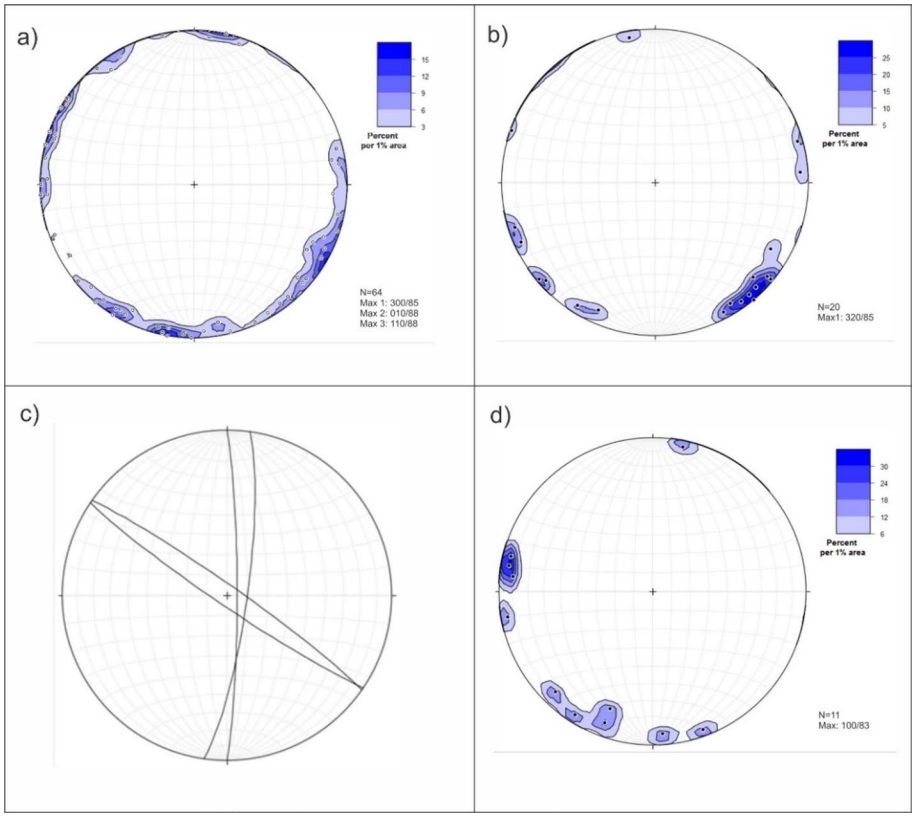

Fig. 5 Pole diagrams and stereograms with data collected at the outcrop. **a** Columnar disjunction, **b** altered basalt, **c** laterite, **d** soil

area, aligned with the axis of the drainage line. The 2D inversions resulted in horizontal sections with resistivity values ranging from 10Ωm to 1500Ωm, which were represented with shades ranging from blue (low resistivity) to red (high resistivity), making it easier to visualize the different geological and hydrogeological zones present at the site (Fig. 6).

The electrical resistivity sections revealed the predominant presence of a zone of high electrical resistivity in the more shallow regions, with values between 733Ωm and over 1500Ωm, extending up to 960 m. This zone was interpreted as an unsaturated region, possibly associated with the soil during the dry season or poorly altered rocks with a low degree of fracturing. Punctual areas of very high electrical resistivity, above 1500Ωm, were observed on the flanks of the valley, at distances of up to 80 m on the northeast (NE) side and from 320 m on the southwest (SW) side, showing specific geological characteristics that may be related to the presence of more compact rocks or geological structures that affect the distribution of groundwater. Just below the most resistive zone, a region with low electrical resistivity values was identified, ranging from 10Ωm to 41.9Ωm, which occurs from the 970 m elevation and extends to the depths investigated. This low resistivity zone is typical of areas saturated with groundwater, suggesting that the region below this elevation is characterized by a high moisture content, which reflects the presence of water in the subsoil. In the lower central portion, from the 940 m elevation onwards, the electrical resistivity values increase again, varying between 85.6Ωm and 358Ωm, indicating a transition zone between unsaturated material and the water-saturated zone, where medium to high resistivity values are associated with soils

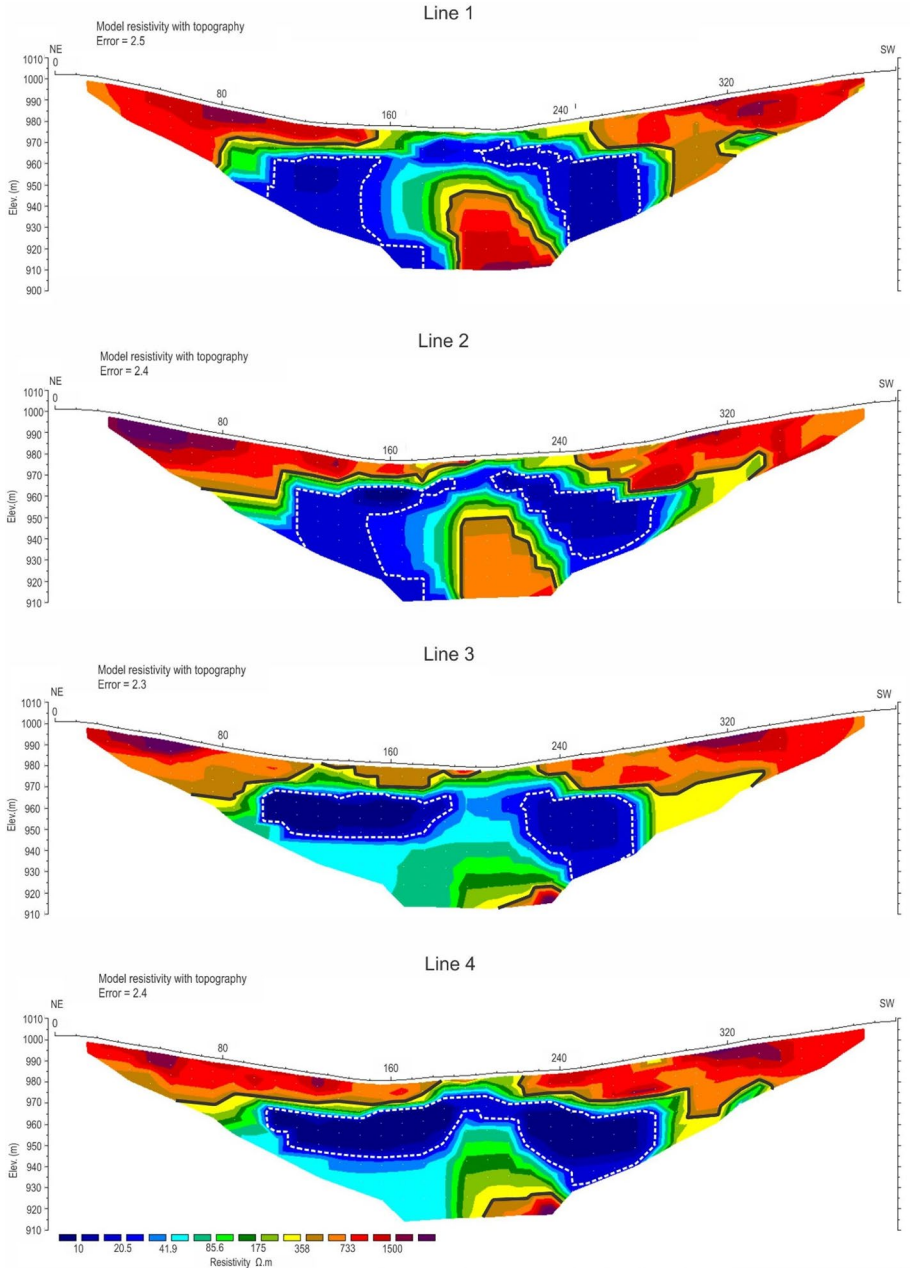

Fig. 6 2D inversion models of electrical resistivity tomography lines. White traces surround the saturated area and the black line the unsaturated zone

or rocks which, although still unsaturated, are beginning to show distinct characteristics from the more superficial zone.

The elevations of the edges of the valley remain constant along the measurement lines, while the center, corresponding to the drainage line, shows a variation of 10 m between line 1 (980 m) and line 7 (990 m). This topographic variation in elevation is important as it can influence the interpretation of local hydrogeological conditions. On lines 1, 2 and 7, it was possible to observe the shape of the reservoir, with less resistive zones concentrated on the flanks and connecting in a restricted way just below the drainage line, while the most resistive zones were observed at the top and below, in the center. Sections 3, 4, 5 and 6 showed that the most electrically resistive zone below the center has a

rectilinear pattern, suggesting the presence of a geological structure, possibly a fracture, which may be influencing the connections between the two bodies of groundwater identified (Fig. 7).

In Line T, the continuity of the zone of low electrical resistivity and the rectilinear displacement observed suggest the presence of a geological structure, possibly a reverse fault with a NE-SW direction. This structural pattern, together with the orientation of the drainage line (SE-NW), suggests that the underground flow to the north of the fault runs in a NW direction, while to the south it moves SE, towards the front of the cuesta. This configuration indicates that the fault may act as a barrier to groundwater flow, controlling the direction and distribution of water in the subsoil. In order to better

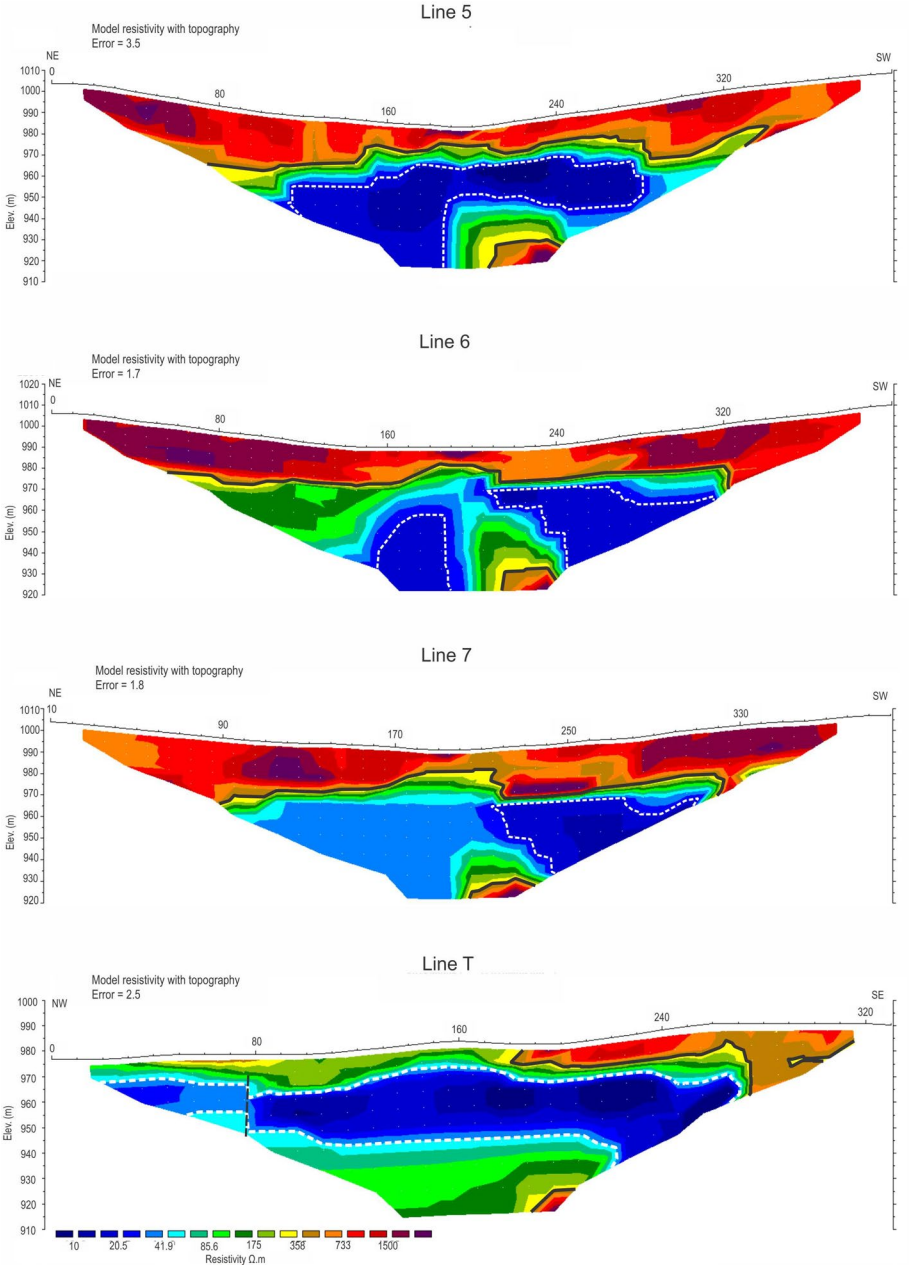

Fig. 7 2D inversion models of electrical resistivity tomography lines. White traces surround the saturated area and the black line the unsaturated zone. Black dashes on the T line represent a fault

understand the hydrogeological dynamics of the area, three-dimensional models of electrical resistivity variations were generated by interpolating the data obtained from the 8 ERT lines. These models provided a better view of the spatial distribution of electrical resistivity and allowed better observation of the boundary between the saturated and unsaturated zones, as well as the influence of geological structures on underground flow (Fig. 7).

5 Discussions

Processing the sections generated 3D block models (Fig. 8), which revealed important patterns in the distribution of electrical resistivity in the area. The most electrically resistive areas were observed at the top and bottom of the model, with a narrower center. The portions with low resistivity, located mainly at the edges, continue beyond the maximum depth investigated, suggesting a significant extension of these zones into the subsoil.

In Fig. 9, with a top view, it is possible to identify two main bodies of lower resistivity, about 300 m long, connected in the southwest region. The center of the model has a higher resistance, especially in the NW direction, while the structures with low resistivity are aligned in the NW-SE direction, which may indicate the presence of fractures or other geological zones of hydrogeological interest.

For a more detailed analysis, a 3D image was generated with a NW to SE view, clearly showing the shape of the aquifer reservoir. In this model, it can be seen that the two bodies of water are more extensive, while the center, where the connections occur, is more restricted. Figure 10 illustrates the cycle of recharge and discharge of the aquifer, with

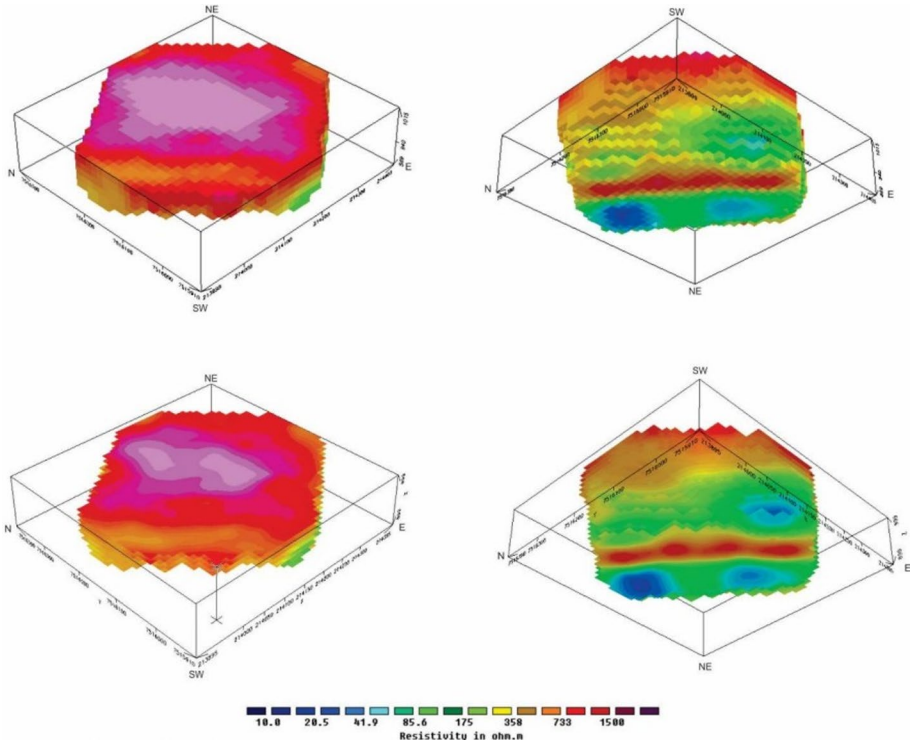

Fig. 8 3D block models generated from the electrical resistivity sections, illustrating the spatial distribution of resistivity variations in the study area. The most resistive areas are located at the top and bottom, with zones of low resistivity, which indicate the presence of groundwater, visible at the edges and continuing beyond the maximum depth investigated

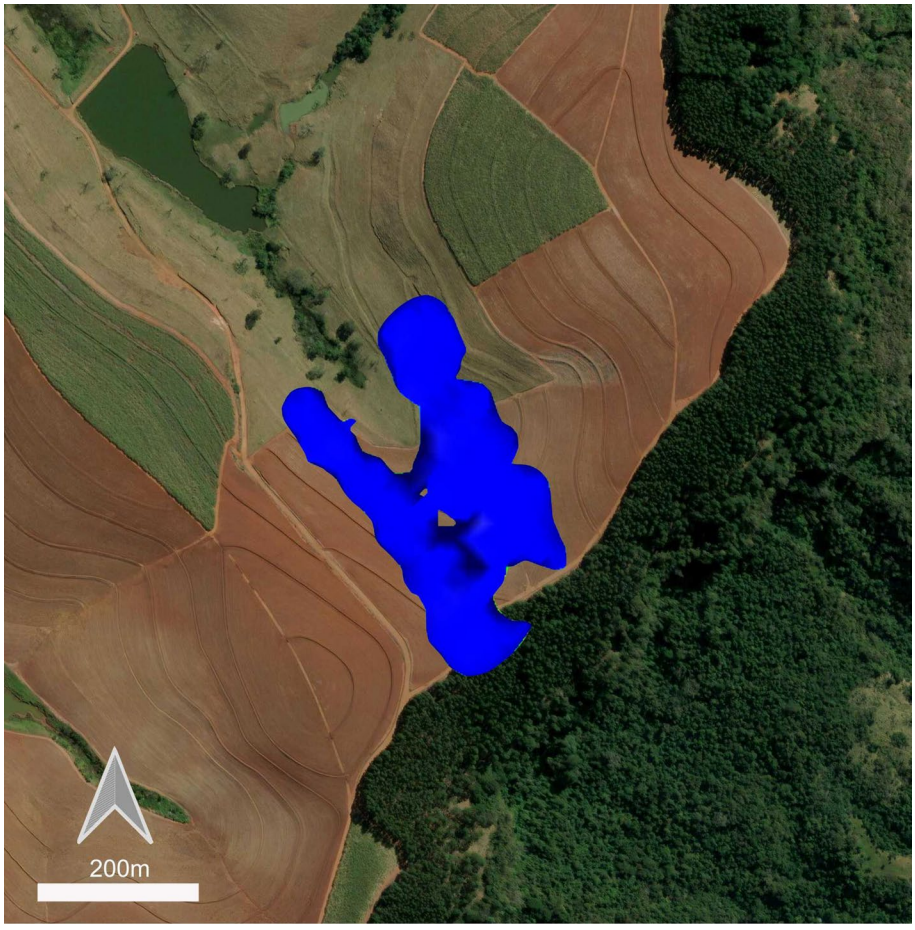

Fig. 9 Aerial view of the 3D model of the area studied, showing the main bodies of low electrical resistivity. The zones of low resistivity are visible for approximately 300 m, with some connections in the southwest, and the center of the area shows higher resistivity, especially in the NW direction. The alignment of the low resistivity structures follows a NW-SE orientation, reflecting possible geological features such as fractures or faults

the infiltration of water at the surface, represented by arrows, which reaches the free aquifer and continues into the fractured zone, being drained by the drainage lines. A filter was used to highlight the lower resistivity zones, which are more likely to represent wetlands. The continuity of these zones, especially on the left, extends beyond the maximum depth investigated, which suggests that the aquifer may have a significant vertical extension.

In addition to hydrogeological issues related to the area's load and recharge cycle, which are essential for water supply and security, it is important to consider contamination scenarios, especially in areas close to cultivation zones. In regions with intensive agriculture, such as sugar cane plantations, there may be a risk of contamination of the aquifer by substances such as pesticides, fertilizers or other pollutants. These substances can infiltrate the soil and reach the aquifer due to the proximity of the groundwater to the surface, as seen in the sections and Fig. 10, which indicate a considerable thickness of the aquifer and its proximity to the surface during the dry season. The risk of contamination is particularly high in areas where the soil is exposed, as was the case during the fieldwork when the sugar cane plantation was absent, but it can recur at other times. The presence of contaminants such as pesticides and herbicides used in plantations can compromise groundwater quality, posing a

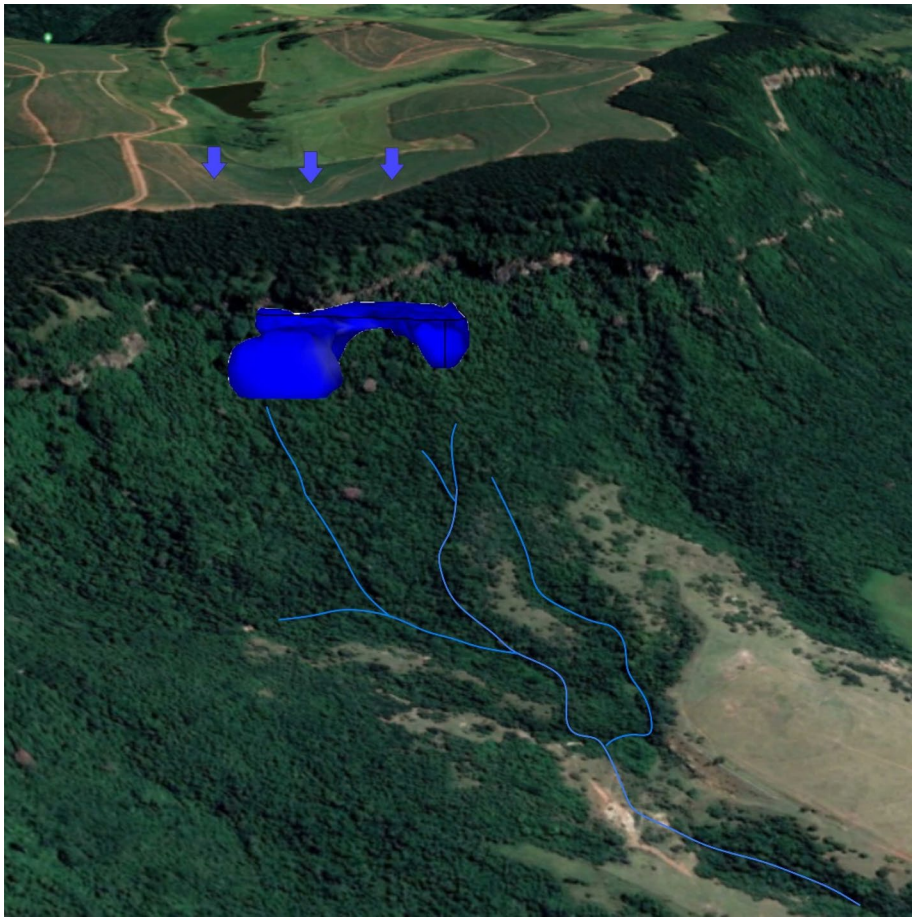

Fig. 10 Three-dimensional model of the aquifer, highlighting the recharge zone (blue arrows), the free aquifer and the discharge zone represented by the drainage lines (blue lines). The model illustrates the path of the infiltrated water from the surface to the aquifer, with the underground flow going into the fractured zones and draining along the drainage lines. Areas of lower electrical resistivity indicate regions potentially saturated with water

significant risk to public health and the environment. This analysis highlights the importance of continuous monitoring of groundwater quality, especially in areas of agricultural cultivation, to ensure the sustainability of water resources and avoid contamination of the aquifer, which can compromise not only the water supply but also the environmental health of the region.

6 Conclusions

This study successfully identified and characterized a fractured confined aquifer in a geologically complex region, primarily composed of sandstones and basalts from the São Bento Group (Serra Geral Formation), overlaid by sedimentary rocks from the Paraná Basin. This geological configuration, typical of transitional environments between sedimentary basins and volcanic terrains, creates ideal conditions for the formation of fractured aquifers and surface recharge zones. These findings underline the area's significance as a natural laboratory for studying hydrogeological behavior in heterogeneous terrains.

The application of electrical resistivity tomography proved to be an efficient and effective tool for aquifer characterization. The Schlumberger array, in particular, demonstrated its ability to correlate depth and lateral extent, producing 2D inversion models that revealed significant electrical resistivity contrasts between saturated and unsaturated zones. Additionally,

the study identified a NE-SW oriented reverse fault, which plays a crucial role in controlling the underground water flow, highlighting the importance of tectonic structures in fractured aquifer systems.

The three-dimensional models further enriched the understanding of the aquifer system, revealing two elongated bodies of water in a NW-SE direction, connected by secondary NE-SW oriented structures. This structural pattern is characteristic of confined aquifer systems in tectonically reactivated terrains, similar to those found in mountainous regions globally. Notably, the aquifer's proximity to the surface and its location at the top of the cuesta indicate its role as a crucial recharge zone, making it particularly vulnerable to anthropogenic pressures, such as intensive agricultural practices involving fertilizers and pesticides.

These findings emphasize the importance of integrating geophysical methods into aquifer characterization and management in areas with similar geological complexity. The approach demonstrated in this study offers a replicable methodology for assessing aquifers in regions of steep relief and high geological heterogeneity. Moreover, the connection between the identified aquifer and the adjacent drainage systems underscores the critical need for protecting recharge zones, which are vital for ensuring the sustainability of regional water resources.

Author contributions
All authors contributed to the conceptualization of the study. CAM: conceived, designed, and conducted the study, analyzed the data, prepared all figures and tables. LGN: contributed to writing the main manuscript text, assisted in the interpretation of geophysical data and prepared all figures and tables. SFS: collected the data, assisted in the interpretation of geophysical data, contributed to writing the main manuscript text and prepared all figures and tables. IAS: analyzed the data and contributed to writing the main manuscript text. HM: analyzed the data and contributed to writing the main manuscript text. MAFH: analyzed the data and contributed to writing the main manuscript text. JPRL: analyzed the data and contributed to writing the revised manuscript text.

Funding
No funding was received.

Data availability
The data that support the findings of this study are available on request from the corresponding author, Guireli Netto, L.

Declarations

Ethics and consent to participate
Not applicable.

Competing interests
The authors declare no competing interests.

Received: 7 January 2025 / Accepted: 16 June 2025
Published online: 21 June 2025

References

1. UNESCO. (2015). The United Nations world water development report: water for a sustainable world. UNESCO. https://unesdoc.unesco.org/ark:/48223/pf0000231823
2. Grönwall J, Danert K. Regarding groundwater and drinking water access through A human rights lens: Self-Supply as A norm. Water. 2020;12(2):419. https://doi.org/10.3390/w12020419.
3. Pointet T. The united nations world water development report 2022 on groundwater, a synthesis. LHB. 2022;108(1). https://doi.org/10.1080/27678490.2022.2090867.
4. Elumalai P, Gao X, Parthipan P, Luo J, Cui J. Agrochemical pollution: a serious threat to environmental health. Curr Opin Environ Sci Health. 2025. https://doi.org/10.1016/j.coesh.2025.100597.
5. Dutton AR. (2015). Hydrogeology: principles and practice, 2nd edition. Groundwater, 53: 830–831. https://doi.org/10.1111/gwat.12374
6. Delaunay N, Marques ED, Nummer AR, Kutter VT, Silva-Filho EV, Lage IC. Hydrogeochemical characterization and indicators of anthropogenic influence in groundwater around Guanabara bay, Rio de janeiro, Brazil. J South Am Earth Sci. 2024. https://doi.org/10.1016/j.jsames.2024.105175.
7. Sethi R, Di Molfetta A. Aquifer vulnerability and contamination risk. Groundwater engineering. Springer Tracts in Civil Engineering. Cham: Springer; 2019. https://doi.org/10.1007/978-3-030-20516-4_7.
8. Ashraf B, AghaKouchak A, Alizadeh A, et al. Quantifying anthropogenic stress on groundwater resources. Sci Rep. 2017;7:12910. https://doi.org/10.1038/s41598-017-12877-4.

9. Fan Y. Groundwater in the earth's critical zone: relevance to large-scale patterns and processes. Water Resour Res. 2015;51:3052–69. https://doi.org/10.1002/2015WR017037.
10. Benz SA, Irvine DJ, Rau GC, et al. Global groundwater warming due to climate change. Nat Geosci. 2024;17:545–51. https://doi.org/10.1038/s41561-024-01453-x.
11. Gomes MAF. Uso agrícola Das áreas de afloramento do Aquífero Guarani no brasil: implicações Para a Água subterrânea e propostas de Gestão com enfoque agroambiental. Brasília: EMBRAPA; 2008. p. 417.
12. Oliveira M, Moreira CA, Guireli Netto L, Nascimento M, Sampaio B. Geophysical and geological surveys to understand the hydrogeological behavior in an outcrop area of the Guarani aquifer system, in Brazil. Environ Challenges. 2022;6:100448. https://doi.org/10.1016/j.envc.2022.100448.
13. Aquilina L, Stumpp C, Tonina D, Buffington JM. (2023). 1 Hydrodynamics and geomorphology of groundwater environments. https://doi.org/10.1016/B978-0-12-819119-4.00014-7
14. Maliva RG. Fractured sedimentary rock aquifers. Aquifer characterization techniques. Springer hydrogeology. Cham: Springer; 2016. https://doi.org/10.1007/978-3-319-32137-0_17.
15. Singha K, Day-Lewis FD, Johnson T, Slater LD. Advances in interpretation of subsurface processes with time-lapse electrical imaging. Hydrol Process. 2015;29:1549–76. https://doi.org/10.1002/hyp.10280.
16. Moreira CA, Netto LG, de Siqueira Buchi FM, et al. Using electrical resistivity tomography to understand the hydrogeological behavior of acid drainage percolation in a fractured aquifer at a uranium mining site. Mine Water Environ. 2024;43:431–48. https://doi.org/10.1007/s10230-024-00998-y.
17. Barbosa AM, Netto LG, Guimarães CC, et al. Geoenvironmental and geophysical methods applied to identify natural Attenuation process on a complex hydrogeological environment contaminated by hydrocarbons. Discov Environ. 2024;2:123. https://doi.org/10.1007/s44274-024-00158-7.
18. Dumont M, Singha K. Geophysics as a hypothesis-testing tool for critical zone hydrogeology. WIREs Water. 2024;11(5):e1732. https://doi.org/10.1002/wat2.1732.
19. Akpan AE, Ekwok SE, Ben UC, Ebong ED, Thomas JE, Ekanem AM, George NJ, Abdelrahman K, Fnais MS, Eldosouky AM, Andráš P, Alarifi SS. Direct detection of groundwater accumulation zones in Saprock aquifers in Tectono-Thermal environments. Water. 2023;15(22):3946. https://doi.org/10.3390/w15223946.
20. Moreira CA, Helene LPI. Identification for a favorable area of groundwater exploitation based on structural and geoelectrical data in fractured aquifer in Southern Brazil. Geofísica Int. 2022;61:287–300. https://doi.org/10.22201/igeof.00167169p.2022.61.4.2045.
21. Sreeparvathy V, Kambhammettu BVNP, Peddinti SR, Sarada PSL. Application of ERT, saline tracer and numerical studies to delineate Preferential paths in fractured granites. Groundwater. 2019;57:126–39. https://doi.org/10.1111/gwat.12663.
22. Szalai S, Kovács A, Kuslits L, Facskó G, Gribovszki K, Kalmár J, Szarka L. Characterisation of fractures and fracture zones in a carbonate aquifer using electrical resistivity tomography and pricking probe methodes. J Geosci Environ Protect. 2018;6:1–21. https://doi.org/10.4236/gep.2018.64001.
23. Nugraha GU, Bakti H, Lubis RF, et al. Aquifer vulnerability in the coastal northern. Part of Lombok Island Indonesia. Environ Dev Sustain. 2022;24:1390–410. https://doi.org/10.1007/s10668-021-01459-0.
24. Pradhan RM, Guru B, Pradhan B, Biswal TK. Integrated multi-criteria analysis for groundwater potential mapping in precambrian hard rock terranes (North Gujarat), India. Hydrol Sci J. 2021;66(6):961–78. https://doi.org/10.1080/02626667.2021.1906427.
25. Falade AH, Olajuyigbe OE, Oni AG, et al. Integrated magnetic and electrical resistivity investigation for assessment of the causes of road pavement failure along the Ife-Osogbo highway, Southwestern Nigeria. Model Earth Syst Environ. 2021;7:1425–41. https://doi.org/10.1007/s40808-020-00966-9.
26. Faleye ET, Olorunfemi MO, Bamidele OE, et al. Remote sensing and geophysical mapping of lineaments and evaluation of the hydrogeological significance: a case study for the Ipogun drainage basin, Southwestern Nigeria. Sustain Water Resour Manag. 2025;11:37. https://doi.org/10.1007/s40899-025-01216-5.
27. Ebong ED, Emeka CN, Melouah O, Ullah RI, Ita AE, Asfahani J. Delineation of groundwater potential zones using electrical resistivity technique in Obudu basement terrain of cross river state, southeastern Nigeria. Water Pract Technol. 2023;2884–900. https://doi.org/10.2166/wpt.2023.174.
28. Ebong ED, Akpan AE, Onwuegbuche AA. Estimation of geohydraulic parameters from fractured shales and sandstone aquifers of abi (Nigeria) using electrical resistivity and hydrogeologic measurements. J Afr Earth Sc. 2014;96:99–109. https://doi.org/10.1016/j.jafrearsci.2014.03.026.
29. Ebong ED, Akpan AE, Emeka CN, Urang JG. (2017). Groundwater quality assessment using geoelectrical and geochemical approaches: case study of Abi area, southeastern Nigeria. Appl Water Sci 7, 2463–2478 (2017). https://doi.org/10.1007/s13201-016-0439-7
30. Ekwok SE, Akpan AE, Kudamnya EA, Ebong ED. Assessment of groundwater potential using geophysical data: a case study in parts of cross river state, south-eastern Nigeria. Appl Water Sci. 2020;10:144. https://doi.org/10.1007/s13201-020-01224-0.
31. Odong PO, Ebong ED, Awak EA, Ojong RA, Umera RB. Integrated geophysical and hydrogeochemical characterization of groundwater vulnerability conditions in part of Ikom-Mamfe embayment, southeastern Nigeria. Sustain Water Resour Manag. 2024;10:120. https://doi.org/10.1007/s40899-024-01094-3.
32. Ducut JD, Alipio MI, Go PJ, Concepcion RS, Vicerra RR, Bandala AA, Dadios EP. A review of electrical resistivity tomography applications in underground imaging and object detection. Displays. 2022;73:102208. https://doi.org/10.1016/j.displa.2022.102208.
33. Lee SC, Noh KA, Zakariah MN. High-resolution electrical resistivity tomography and seismic refraction for groundwater exploration in fracture hard rocks: A case study in kanthan, perak, Malaysia. J Asian Earth Sci. 2021;218:104880. https://doi.org/10.1016/j.jseaes.2021.104880.
34. Takele T, Husein M, Diriba D, Assefa G. Application of electrical resistivity tomography for groundwater evaluation in Yirgacheffe town and its environs, main Ethiopian rift. HydroResearch. 2024. https://doi.org/10.1016/j.hydres.2024.11.003.
35. Imani P, Tian G, Hadiloo S, El-Raouf AA. Application of combined electrical resistivity tomography (ERT) and seismic refraction tomography (SRT) methods to investigate Xiaoshan district landslide site: hangzhou, China. J Appl Geophys. 2021. https://doi.org/10.1016/j.jappgeo.2020.104236.

36. Jasrotia AS, Sharma A, Ahmad S, et al. Aquifer characterization and evaluation of groundwater potential zones in the frontal part of the Himalayas using electrical resistivity tomography technique. J Earth Syst Sci. 2025;134:18. https://doi.org/10.1007/s12040-024-02467-0.
37. Albuquerque GM, Mansur KL, Silva GC, Mello CL, Braga MA. Fault mapping and characterization of a coastal aquifer related to a Mangrove ecosystem, using electrical resistivity tomography (ERT), ground penetrating radar (GPR) and hydrochemical data: the case of the Mangue de Pedra aquifer, Armação Dos búzios, Brazil. J South Am Earth Sci. 2022. https://doi.org/10.1016/j.jsames.2022.104095.
38. Ogura AP, Da Silva AC, Castro GB, Espíndola EL, Da Silva AL. An overview of the sugarcane expansion in the state of São Paulo (Brazil) over the last two decades and its environmental impacts. Sustainable Prod Consum. 2022. https://doi.org/10.1016/j.spc.2022.04.010.
39. Meles MB, Bradford SA, Casillas-Trasvina A, Chen L, Osterman G, Hatch T, Ajami H, Crompton OV, Levers L, Kisekka I. Uncovering the gaps in managed aquifer recharge for sustainable groundwater management: A focus on hillslopes and mountains. J Hydrol. 2024. https://doi.org/10.1016/j.jhydrol.2024.131615.
40. Scanlon BR, Fakhreddine S, Rateb A, et al. Global water resources and the role of groundwater in a resilient water future. Nat Rev Earth Environ. 2023;4:87–101. https://doi.org/10.1038/s43017-022-00378-6.
41. Milani EJ, Melo JHG, Souza PA, Fernandes LA, França AB. (2007). Bacia do Paraná. Boletim de Geociências da Petrobras, 15(2), 265–287. Retrieved from https://bgp.petrobras.com.br/bgp/article/view/310
42. Perrotta MM, Salvador ED, Lopes RdaC, Agostino D, Chieregati LZ, Peruffo LA, Gomes N, Sachs SD, Meira LLB, da Garcia VT G. M., de Lacerda Filho JV. (2006). *Mapa geológico e de recursos minerais do estado de São Paulo (1:750.000)*. Serviço Geológico do Brasil (CPRM). Retrieved from https://rigeo.sgb.gov.br/handle/doc/2966
43. Fernandes MA, dos Reis Fernandes LB, Schutzer JB. Desert cretaceous dinosaurs: the Botucatu paleodesert and the footprints across the dunes. In: Carvalho IS, Leonardi G, editors. Dinosaur tracks of mesozoic basins in Brazil. Cham: Springer; 2024. https://doi.org/10.1007/978-3-031-56355-3_4.
44. Tamrat E, Ernesto M. Paleomagnetic constraints on the age of the Botucatu formation in Rio Grande do sul, Southern Brazil. An Acad Bras Cienc. 2006;78(3):591–605. https://doi.org/10.1590/S0001-37652006000300016.
45. Renne PR, Ernesto M, Pacca IG, Coe RS, Glen JM, Prévot M, Perrin M. The age of Paraná flood volcanism, rifting of gondwanaland, and the Jurassic-Cretaceous boundary. Science. 1992;258(5083):975–9. https://doi.org/10.1126/science.258.5084.97.
46. Milani EJ. Evolução tectono-estratigráfica Da Bacia do Paraná e Seu relacionamento com a geodinâmica fanerozóica do Gondwana Sul-ocidental. Tese de doutorado. Brasil: Universidade Federal do Rio Grande do Sul, Porto Alegre; 1997.
47. Liu CC. (1984). Análise estrutural de lineamentos em imagens de sensoriamento remoto: Aplicação ao Estado do Rio de Janeiro (Doctoral dissertation). Instituto de Geociências, Universidade de São Paulo, São Paulo, Brazil. Retrieved from https://teses.usp.br/teses/disponiveis/44/44131/tde-25082015-143959/pt-br.php
48. Griffiths DH, Barker RD. Two-Dimensional resistivity imaging and modeling in areas of complex geology. J Appl Geophys. 1993;29:21–6. 10.1016/0926–9851(93)90005-J.
49. Binley A, Kemna A. DC resistivity and induced polarization methods. In: Rubin Y, Hubbard SS, editors. *Hydrogeophysics*. Water science and technology library. Volume 50. Dordrecht: Springer; 2005. https://doi.org/10.1007/1-4020-3102-5_5.
50. Netto LG, Moreira CA, Bianchi HM, et al. Characterization of excavated radionuclide retention ponds in a uranium mine in the process of decommissioning using geophysical methods. Pure Appl Geophys. 2024;181:3313–30. https://doi.org/10.1007/s00024-024-03602-0.
51. Rebés Lima JP, Corrêa ICS, Weschenfelder J, et al. Geoelectric subsurface characterization in the emerged portion of the Barra Falsa channel using the ground conductivity meter (LIN-EM), bojuru, RS, Brazil. Geofísica Int. 2025;64(1):1417–35. https://doi.org/10.22201/igeof.2954436xe.2025.64.1.1747.
52. Xu D, Hu X, Zha Y, Yeh TJ. Exploiting electrical resistivity tomography for hydraulic tomography: sandbox experiments. Adv Water Resour. 2024. https://doi.org/10.1016/j.advwatres.2024.104778.
53. Ritchie H, Holman I, Nyangoka J, Bauman P, Parker A. Insights from electrical resistivity tomography on the hydrogeological interaction between sand dams and the weathered basement aquifer. J Appl Geophys. 2024. https://doi.org/10.1016/j.jappgeo.2024.105542.
54. Rangel R, Porsani J, Bortolozo C, Hamada L. Electrical resistivity tomography and TDEM applied to hydrogeological study in Taubaté basin, Brazil. Int J Geosci. 2018;9:119–30. https://doi.org/10.4236/ijg.2018.92008.
55. Moreira CA, Lapola MM, Carrara A. Comparative analyzes among electrical resistivity tomography arrays in the characterization of flow structure in free aquifer. Geofísica Int. 2016;55(2):119–29.
56. Telford WM, Geldart LP, Sheriff RE. Applied geophysics. 2nd ed. Cambridge University Press; 1990.
57. ABEM. (2012). Terrameter LS Instruction Manual. https://wwwguidelinegeoc.cdn.triggerfish.cloud/uploads/2016/03/User-Guide-Terrameter-LS-2012-10-25.pdf
58. Günther T, Rücker C, Spitzer K, Inversion, Geophys J Int. 2006;166(2):506–517. https://doi.org/10.1111/j.1365-246X.2006.03011.x
59. Dahlin T, Loke MH. Resolution of 2D Werner resistivity imaging as assessed by numerical modelling. J Appl Geophys. 1998;38(4):237–49. https://doi.org/10.1016/S0926-9851(97)00030-X.
60. Ebong ED, Abong AA, Ulem EB, et al. Geoelectrical resistivity and geological characterization of hydrostructures for groundwater resource appraisal in the Obudu plateau, southeastern Nigeria. Nat Resour Res. 2021;30:2103–17. https://doi.org/10.1007/s11053-021-09818-4.
61. Shawky MM. A comparative study of interpolation methods for the development of ore distribution maps. Discov Geosci. 2025;3. https://doi.org/10.1007/s44288-025-00108-7. 2.
62. Hasui Y. Neotectônica e aspectos fundamentais da tectônica ressurgente no Brasil. In: Workshop sobre neotectônica e sedimentação cenozoica continental no sudeste brasileiro. 1990; pp. 1–31.
63. Riccomini C, Assumpção M. Quaternary tectonics in Brazil. Episodes. 1999;22(3):221–5. https://doi.org/10.18814/epiiugs/1999/v22i3/010.

Publisher's note